An Optimized Numerical Method for Solving the Two-Dimensional Impedance Equation

C. M. A. Robles G. *IAENG, Member*, A. Bucio R. and M. P. Ramirez T. *IAENG, Member*.

***Abstract*—We study an optimized numerical method for solving the forward problem of the two-dimensional Impedance Equation. Based upon elements of the modern Pseudoanalytic Function Theory, its performance is tested employing sinusoidal conductivity functions within the unit circle. Then a collection of experimental data are displayed for illustrating its effectiveness. The work closes with a brief discussion of the contribution to the Electrical Impedance Tomography problem.**

***Index Terms*—Computational method, Electrical Impedance Equation, Pseudoanalytic Function Theory.**

I. Introduction

THE elements of the modern Pseudoanalytic Function Theory [7], have been successfully applied for sorting out the forward problem of the Impedance Equation in the plane

$$\operatorname{div}(\sigma \operatorname{grad} u) = 0, \tag{1}$$

where σ is the conductivity and u is the electric potential. Specifically, when σ can be expressed as a separable-variables function, it is possible to approach the general solution of (1) in asymptotic form, harnessing Taylor series in formal powers [2].

Nevertheless, the application of this technique may have some restrictions when dealing with engineering problems, because the conductivity functions rising from experimental models, in general, do not posses a separable-variables structure. An alternative for overpassing this restriction was posed in [9], where it was shown that, under certain circumstances, every physical-rising conductivity distribution, can be considered a limit case of a piecewise separable-variables function.

The relevance of efficiently solving the forward problem for (1), if we are to solve the Electrical Impedance Tomography problem (also called inverse problem), was widely exposed in a variety of works, among which [12] is one of the most important. In this sense, the results posed in [8], and subsequently rediscovered in [1], are indeed very significant, because they allowed to sift out the rink for approaching the general solution of the Impedance Equation in the plane.

After publishing these works, many interesting papers, dedicated to numerically solving the Dirichlet boundary value problem of (1) in the plain, have achieved to approach the solutions with considerable accuracy (see e.g. [6]).

The main contribution of this work is to propose an efficient numerical method, whose algorithm displays an adequate valance between the computational cost and accuracy.

C. M. A. Robles G. is with the National Polytechnique Institute, ESIME C. Mexico, cesar.robles@lasallistas.org.mx

A. Bucio R. is with the National Polytechnique Institute, UPIITA, Mexico, ari.bucio@gmail.com

M. P. Ramirez T. is with the Communications and Digital Signal Processing Group, Engineering Faculty of La Salle University, Mexico, marco.ramirez@lasallistas.org.mx.

We shall remark once more that many of the existing methods are highly accurate, but they engross the usage of computational resources, and also impose mathematical restrictions that locate them far away from engineering applications. The method posed in the following paragraphs may avoid these problems, becoming appropriate for, e.g., analysing Electrical Impedance Tomography problems upcoming from clinical cases.

Hence, we first broach a simplified numerical method for solving (1) at the boundary of some domain in the plain [3]. This is done by approaching elements of a complete set of solutions for a Vekua equation [11], fully equivalent to (1). Then we examine a special class of examples, in order to illustrate the effectiveness of the method, lodging an explanation of its performance through a set of control parameters. The conclusions contain the arguments that might justify the viability of employing this new technique.

II. Preliminaries

According to the Pseudoanalytic Function Theory posed in [2], let us consider a pair of complex-valued functions (F, G) that fulfil the condition

$$\operatorname{Im}\left(\overline{F}G\right) > 0, \tag{2}$$

where $\overline{F}$ denotes the complex conjugate of F:

$$\overline{F} = \mathrm{Re}F - i\mathrm{Im}F.$$

Thus, any complex function W can be expressed by the linear combination of F and G:

$$W = \phi F + \psi G,$$

where ϕ and ψ are real-valued functions.

A pair (F, G) that heeds (2) is named a *generating pair*. This concept allowed L. Bers to introduce the (F, G)-derivative of a function W:

$$\partial_{(F,G)} W = (\partial_z \phi) F + (\partial_z \psi) G, \tag{3}$$

where $\partial_z = \frac{\partial}{\partial x} - i\frac{\partial}{\partial y}$, and $i^2 = -1$. This derivative will only exist if

$$(\partial_{\overline{z}} \phi) F + (\partial_{\overline{z}} \psi) G = 0, \tag{4}$$

where $\partial_{\overline{z}} = \frac{\partial}{\partial x} + i\frac{\partial}{\partial y}$.

Moreover, when introducing the notations

$$A_{(F,G)} = \frac{\overline{F}\partial_z G - \overline{G}\partial_z F}{F\overline{G} - \overline{F}G}, \quad B_{(F,G)} = \frac{F\partial_z G - G\partial_z F}{F\overline{G} - \overline{F}G},$$
$$a_{(F,G)} = \frac{\overline{G}\partial_{\overline{z}} F - \overline{F}\partial_{\overline{z}} G}{F\overline{G} - \overline{F}G}, \quad b_{(F,G)} = \frac{F\partial_{\overline{z}} G - G\partial_{\overline{z}} F}{F\overline{G} - \overline{F}G}; \tag{5}$$

the equation (3) can be written as

$$\partial_{(F,G)} W = \partial_z W - A_{(F,G)} W - B_{(F,G)} \overline{W}, \tag{6}$$

ISBN: 978-988-19251-6-9
ISSN: 2078-0958 (Print); ISSN: 2078-0966 (Online)

forasmuch (4) attains

$$\partial_{\overline{z}} W - a_{(F,G)} W - b_{(F,G)} \overline{W} = 0. \tag{7}$$

Concretely, the notations (5) are called the *characteristic coefficients* of the generating pair (F, G). The expression (6) is referred as the (F, G)-derivative of W, and (7) is the Vekua equation [11].

Remark 1: The functions

$$F = p, \quad G = \frac{i}{p}, \tag{8}$$

where p is a non-vanishing real-valued function, within some domain Ω, makes up a Bers generating pair since they satisfy (2), and their characteristic coefficients are:

$$\begin{aligned} A_{(F,G)} &= a_{(F,G)} = 0, \\ B_{(F,G)} &= -\tfrac{\partial_z p}{p}, \quad b_{(F,G)} = -\tfrac{\partial_{\overline{z}} p}{p}. \end{aligned} \tag{9}$$

Definition 1: Let us suppose that (F_0, G_0) and (F_1, G_1) are two generating pairs with the form (8), and let their characteristics coefficients (5) fulfil the relations

$$B_{(F_0,G_0)} = -b_{(F_1,G_1)}.$$

Then (F_1, G_1) will be called a *successor* pair of (F_0, G_0), and (F_0, G_0) will be a *predecessor* of (F_1, G_1).

Definition 2: Let us consider a set of generating pairs $\{(F_n, G_n)\}$, $n = 0, \pm 1, \pm 2, ...$ such that each (F_n, G_n) is a predecessor of (F_{n+1}, G_{n+1}). The set will be then called a *generating sequence*. If $(F, G) = (F_0, G_0)$, we say that (F, G) is embedded into $\{(F_n, G_n)\}$. Furthermore, if there exist a number k such that $(F_{n+k}, G_{n+k}) = (F_n, G_n)$, we assert that the generating sequence is *periodic*, with a period of magnitude k.

Remark 2: Let us consider a generating pair of the form (8). If p is a separable-variables function

$$p = p_1(x) \cdot p_2(y), \tag{10}$$

the pair will be embedded into a periodic generating sequence, with period $k = 2$, being

$$F_m = p_1(x) p_2(y), \quad G_m = \frac{i}{p_1(x) p_2(y)},$$

when m is even, and

$$F_m = \frac{p_2(y)}{p_1(x)}, \quad G_m = i \frac{p_1(x)}{p_2(y)},$$

when m is odd.

The concept of the (F_0, G_0)-integral was also introduced by professor L. Bers [2].

Definition 3: The adjoint generating pair (F_0^*, G_0^*) corresponding to (F_0, G_0) with the form (8), is defined as:

$$F_0^* = -iF_0, \quad G_0^* = -iG_0. \tag{11}$$

Definition 4: The (F_0, G_0)-integral of a complex valued function W is defined as:

$$\int_{z_0}^{z} W d_{(F_0,G_0)} z = F_0 \mathrm{Re} \int_{z_0}^{z} G_0^* W dz + G_0 \mathrm{Re} \int_{z_0}^{z} F_0^* W dz.$$

Specifically, since the (F_0, G_0)-integral of the (F_0, G_0)-derivative of W reaches

$$\int_{z_0}^{z} \partial_{(F_0,G_0)} W d_{(F_0,G_0)} z = W - \phi(z_0) F_0 - \psi(z_0) G_0, \tag{12}$$

and considering that [2]

$$\partial_{(F_0,G_0)} F_0 = \partial_{(F_0,G_0)} G_0 = 0,$$

the integral expression (12) can be considered the (F_0, G_0)-*antiderivative* of the function $\partial_{(F_0,G_0)} W$.

We refer the reader to the specialized literature [2] and [7], for a detailed description about the existence of the (F_0, G_0)-antiderivative. Hereafter, when this concept is evoked, every complex-valued function will be (F_0, G_0)-integrable by definition.

A. Formal Powers

Professor L. Bers [2] generalized the classical result for expanding any analytic function in Taylor series, for the set of the so-called Pseudoanalytic Functions, by midst of what he introduced as *formal powers*.

Definition 5: The formal power $Z_m^{(0)}(a_0, z_0; z)$ with complex constant coefficient a_0, center at z_0, depending upon z, formal exponent 0, and corresponding to the generation pair (F_m, G_m), is expressed as:

$$Z_m^{(0)}(a_0, z_0; z) = \lambda_m F_m + \mu_m G_m,$$

where λ_m and μ_m are real constants, fulfilling the condition

$$\lambda_m F_m(z_0) + \mu_m G_m(z_0) = a_0.$$

The higher exponents of the formal powers are defined according the recursive formulas

$$\begin{aligned} &Z_{m+1}^{(n+1)}(a_n, z_0; z) = \\ &= (n+1) \int_{z_0}^{z} Z_m^{(n)}(a_0, z_0; z) d_{(F_m,G_m)} z. \end{aligned} \tag{13}$$

Dwell that these integrals operators are indeed (F_m, G_m)-antiderivatives, and every formal power of the set

$$\left\{ Z_m^{(n)}(a_n, z_0; z) \right\}_{n=0}^{\infty},$$

is an (F_m, G_m)-pseudoanalytic function [2].

Employing the previous statements, L. Bers proved that any (F_m, G_m)-pseudoanalytic function can be expressed in *Taylor series in formal powers*

$$W = \sum_{n=0}^{\infty} Z_m^{(n)}(a_n, z_0; z); \tag{14}$$

where

$$a_n = \frac{1}{n!} \partial_{(F_m,G_m)}^{(n)} W(z_0).$$

In this purport, this is an analytical representation of the general solution for the Vekua equation (7).

B. The two-dimensional Impedance Equation

Let us consider the two-dimensional case of the Impedance Equation (1), and let us suppose that the conductivity σ could be expressed in terms of a separable-variable function:

$$\sigma = \sigma_1(x) \cdot \sigma_2(y).$$

Introducing the notations

$$W = \sqrt{\sigma} \left(\frac{\partial}{\partial x} u - i \frac{\partial}{\partial y} u \right), \quad p = \sqrt{\frac{\sigma_2(y)}{\sigma_1(x)}}; \tag{15}$$

ISBN: 978-988-19251-6-9
ISSN: 2078-0958 (Print); ISSN: 2078-0966 (Online)

the Impedance Equation can be written as a Vekua equation

$$\partial_{\overline{z}} W - \frac{\partial_{\overline{z}} p}{p} \overline{W} = 0. \tag{16}$$

Furthermore, as it was elegantly stated in [5], the set

$$\left\{ \mathrm{Re} Z_m^{(n)}(1,0;z)\,|_\Gamma, \quad \mathrm{Re} Z_m^{(n)}(i,0;z)\,|_\Gamma \right\}_{n=0}^{\infty}, \tag{17}$$

conforms a complete system for approaching solutions of the Dirichlet forward problem for (1). Here Γ represents the boundary of the domain Ω, where the formal powers are defined.

In other words, let

$$\begin{gathered} u^{(n)}(1,0,z) = \mathrm{Re} Z_m^{(n)}(1,0;z)\,|_\Gamma, \\ u^{(n)}(i,0,z) = \mathrm{Re} Z_m^{(n)}(i,0;z)\,|_\Gamma; \\ n = 0,1,2,... \end{gathered} \tag{18}$$

If a boundary condition $u|_\Gamma$ is provided, we can always approach it asymptotically

$$\lim_{N\to\infty} \sum_{n=0}^{N} \left(\alpha_n u^{(n)}(1,0,z) + \beta_n u^{(n)}(i,0,z) \right) = u|_\Gamma, \tag{19}$$

where α_j and β_j are real numbers.

This procedure proved its effectiveness in several works (see e.g. [5], [6] and [10]), where the numerical approaches achieved highly accurate results.

Referring the reader to [9], where it was proven that any physical-rising conductivity function, could be considered the limit case of a piece-wise separable-variables function, we will explain the method for numerically approaching a finite set of formal powers with the form (17), in order to solve the forward problem for (1).

III. Formal Power Approaching

Attaching the modern Pseudoanalytic Function Theory studied in [7], to the classical results of [2], we present an improved numerical method that, based onto a previous proposal [3], possesses a higher degree of accuracy and numerical stability. Our explanations will be perform considering the formal powers with coefficients $a_n = 1$, because not any important methodological variation takes place when considering $a_n = i$.

Thence, let us consider a collection of $K+1$ points

$$\{r[k]\}, \ k = 0,1,...,K;$$

equidistantly located in a closed interval $[0,1]$. If the interval $[0,1]$ coincides with a radius R of the unit circle, whose center is $z_0 = 0$, with some specific angle $\theta \in [0, 2\pi)$, we will immediately obtain a collection of points allocated in the plane:

$$\{(x[k], y[k])\}, \ k = 0,1,...K;$$

constructed according to the rule

$$x[k] = r[k]\cos(\theta); \ \ y[k] = r[k]\sin(\theta).$$

Thus the formal powers over such radius R can be approached employing the recursive expressions:

$$\begin{gathered} Z^{(n+1)}[k] = AF[k]\cdot \\ \cdot \mathrm{Re} \sum_{q=0}^{k} \left(G^*[q] Z^{(n)}[q] + G^*[q+1] Z^{(n)}[q+1] \right) \Delta z[q] + \\ + \ AG[k]\cdot \\ \cdot \mathrm{Re} \sum_{q=0}^{k} \left(F^*[q] Z^{(n)}[q] + F^*[q+1] Z^{(n)}[q+1] \right) \Delta z[q], \end{gathered} \tag{20}$$

where

$$\Delta z[q] = x[q+1] - x[q] + i\left(y[q+1] - y[q]\right),$$

and A is a factor that warrants the numerical stability of the method (see [4]). This is, it possesses a direct influence in the convergence and steadiness of the numerical calculations. More precisely, for the examples examined further, we will fix $A = 8$. The absence of the sub-index m in the formal powers shown above, indicates that they all belong to the same generating pair.

In order to display the mathematical operations in an algorithmic format, it will be convenient to denote the operations described in (20) as

$$Z^{(n+1)}[k] = \mathcal{B}\left[Z^{(n)}[k] \right].$$

It is clear that this procedure can be performed for a variety of radii $\{R_s\}$, $s = 1,2,...,S$; each one associated to an angle θ_s belonging to the set

$$\left\{ \theta_1 = 0, \ \theta_2 = \frac{2\pi}{S}, \ \theta_3 = \frac{4\pi}{S}, ..., \theta_S = \frac{2(S-1)\pi}{S} \right\}.$$

We shall also remark that the numerical method was fully developed in *GNU C*, employing an AMD® CPU ATHLON 64-4800 ® at 2.50 GHz.

The Algorithm 1 summarizes the programming details for numerically approaching N formal powers, over S number of radii, and considering $K+1$ points per radius.

Algorithm 1 Boundary value problem solver

$S \leftarrow 1000$; (Number of radii)
$N \leftarrow 40$; (Maximum number of Formal Powers)
$K+1 \leftarrow 1001$; (Number of points per radius)
while $s = 1 \rightarrow S$ **do**
  while $n = 1 \rightarrow N$ **do**
    while $q = 0 \rightarrow K$ **do**
      $Z^{(n+1)}[k] = \mathcal{B}\left[Z^{(n)}[k]\right]$;
    end while
  end while
end while
function ORTHONORMALIZATION
  (Classical Gram-Schmidt Orthonormalization Process)
end function
function APPROACH_BOUNDARY_CONDITION;
  $\sum_{n=0}^{N} \left(\alpha_n u^{(n)}(1,0,z) + \beta_n u^{(n)}(i,0,z) \right)$
end function
save ORTHOGONAL_SYSTEM;
save COEFFICIENTS;

ISBN: 978-988-19251-6-9
ISSN: 2078-0958 (Print); ISSN: 2078-0966 (Online)

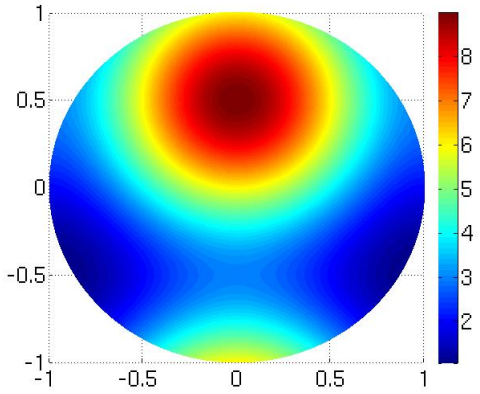

Fig. 1. $\sigma = (2 + \cos(2\hat{\pi}x))\,(2 + \sin(2\hat{\pi}y))$.

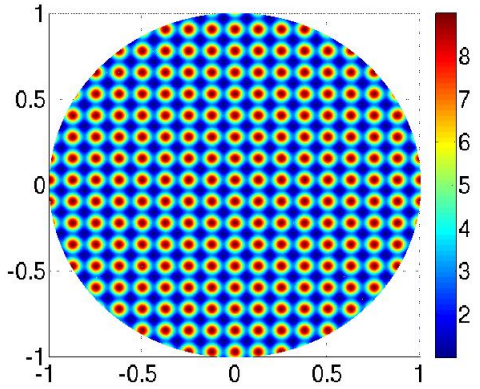

Fig. 2. $\sigma = (2 + \cos(16\hat{\pi}x))\,(2 + \sin(16\hat{\pi}y))$.

IV. Experimental and Results

According to the statements reported in [10], for better illustrating the results obtained employing the method summarized in the Algorithm 1, we selected a conductivity function σ given by a sinusoidal form:

$$\sigma = (2 + \cos(2\tau\hat{\pi}x))\,(2 + \sin(2\tau\hat{\pi}y))\,,\ \tau = \overline{1,8}; \qquad (21)$$

where

$$\hat{\pi} = 3.1416, \qquad (22)$$

since it is not convenient to use a closer approach for the number π, as it will be explained further. This case requires a high degree of accuracy when solving the Dirichlet boundary value problems [10]. The Figure 1 displays the conductivity inside the unitary circle when $\tau = 1$, whereas Figure 2 plots the case when $\tau = 8$.

As the boundary condition, we shall impose an exact solution of (1):

$$\begin{aligned} u = \tfrac{2}{\sqrt{3}} \arctan\left(\tfrac{1}{\sqrt{3}} \tan\left(\hat{\pi}x\right)\right) + \\ + \tfrac{2}{\sqrt{3}} \arctan\left(\tfrac{1}{\sqrt{3}} + \tfrac{2}{\sqrt{3}} \tan\left(\hat{\pi}y\right)\right). \end{aligned} \qquad (23)$$

corresponding to the case when

$$\sigma = (2 + \cos(2\hat{\pi}x))\,(2 + \sin(2\hat{\pi}y))\,.$$

The reason for employing the truncate value (22), is the indetermination of the exact solution (23) when $\hat{\pi} \to \pi$.

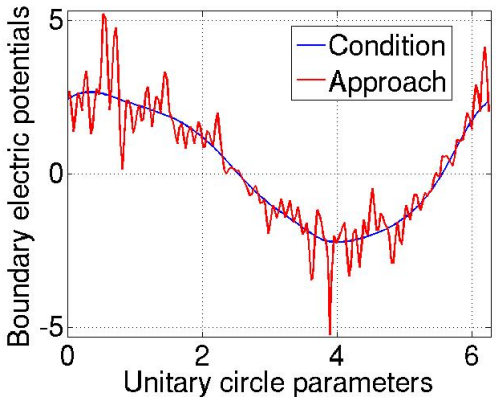

Fig. 3. Approach with $\tau = 8$, $N = 20$, $S = 200$, $K = 200$.

It is easy to verify that the exact solution (23) can not be extended for the cases when $\tau = \overline{2,8}$. Nonetheless, we will continue using it as the boundary condition, for analysing the remaining conductivity functions, in order to stablish a parameter of comparison for examining the behaviour of the method.

For the numerical approached solution at the boundary Γ, we will employ the notation

$$u_{app} = \sum_{n=0}^{N} \left(\alpha_n u^{(n)}\,(1,0,z) + \beta_n u^{(n)}\,(i,0,z)\right). \qquad (24)$$

Thus, the absolute error can be introduced as

$$\mathcal{E} = \left(\int_0^{2\pi} (u|_\Gamma - u_{app})^2 dl\right)^{\frac{1}{2}}, \qquad (25)$$

where $u|_\Gamma$ is in fact the exact solution (23), valued at the perimeter of the unitary circle, and $l \in [0, 2\pi)$.

We compute a set of examples using the conductivities (21), considering different maximum numbers of formal powers N, radii S, and $K+1$ points per radius, whose main results are displayed in the Tables shown bellow.

In order to provide a basic qualitative illustration of the performance, the Figure 3 plots the approached solution for $\tau = 8$, $N = 20$, $S = 200$, and $K = 200$; whereas Figure 4 displays the case when $\tau = 8$, $N = 160$, $S = 1000$, and $K = 200$.

For the first case, the total error was $\mathcal{E} \sim 1.7791$; and for the second case we had an error of $\mathcal{E} \sim 0.0035$. It is remarkable that almost no difference can be appreciated between the curves displayed in Figure 4, corresponding to the approached solution u_{app} and the boundary condition $u|_\Gamma$.

A quantitative perspective is provided in the Tables I and II. The Table I contains the data reached when fixing $\tau = 2$, that, as a matter of fact, corresponds to the case of the Figure 1. Here, it is possible to appreciate that when decreasing the number S of radii, $K+1$ points per radius, and N formal powers, the absolute error $\mathcal{E}$ increases, as it could be expected.

Beside, the Table I illustrates that a relatively low number N of formal powers, can adequately approach the boundary condition $u|_\Gamma$; whereas the increment of points per radius $K+1$ does not significantly impact the diminution of the

ISBN: 978-988-19251-6-9
ISSN: 2078-0958 (Print); ISSN: 2078-0966 (Online)

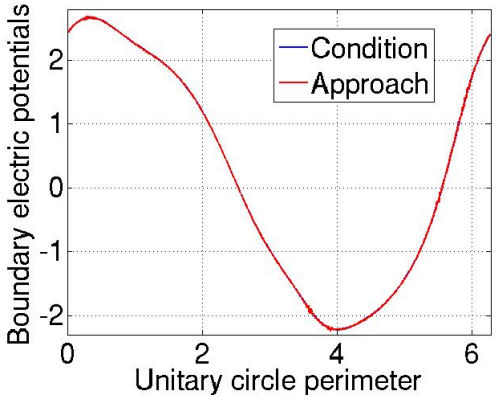

Fig. 4. Approach with $\tau = 8$, $N = 160$, $S = 1000$, $K = 200$.

TABLE I
BRIEF RELATION AMONG PARAMETERS OF THE OPTIMIZED METHOD AND THE ABSOLUTE ERROR $\mathcal{E}$

Radii S	Points $K+1$	Formal Powers N	Error $\mathcal{E}$	Time t (seconds)
1000	1001	40	0.0060	4724.90
1000	1001	35	0.0185	4173.71
1000	1001	30	0.0247	3531.44
1000	1001	25	0.0106	2951.68
1000	1001	20	0.1178	2743.682
800	1001	20	0.1196	3103.35
600	1001	20	0.1427	1507.72
400	1001	20	0.1173	1015.52
200	1001	20	0.0889	481.13
200	801	20	0.0889	308.94
200	601	20	0.0889	180.47
200	401	20	0.0889	78.98
200	201	20	0.0889	20.38

absolute error $\mathcal{E}$, but it considerably increases the computational cost.

On the other hand, the Table II contains the results of fixing the total number of radii at $S = 1000$, and the number of points per radius at $K = 200$. The Table displays an unexpected behaviour, since the absolute error $\mathcal{E}$ does not always decrease at the time the maximum number of formal powers N increases. This phenomenon can be observed in a wide enough variety of arguments for the sinusoidal conductivities.

At this point, the authors are unable to adequately explain the causes of this behaviour, proposing it as an interesting topic for further analysis.

TABLE II
BRIEF RELATION AMONG PARAMETERS OF THE METHOD AND THE ABSOLUTE ERROR $\mathcal{E}$

Formal Powers N	Argument τ	Error $\mathcal{E}$	Time t (seconds)
2	0.5	0.1101	10.70
4	0.5	0.1101	17.75
6	0.5	0.0346	24.81
8	0.5	0.0049	31.84
10	0.5	0.0079	38.87
12	0.5	0.0029	45.97
14	0.5	2.5707×10^{-4}	53.02
16	0.5	1.8248×10^{-4}	60.08
18	0.5	1.0543×10^{-4}	67.41
20	0.5	2.4939×10^{-5}	74.42
20	2	0.1178	74.45
22	2	0.0524	81.52
24	2	0.0508	88.69
26	2	0.0125	95.38
28	2	0.0180	102.26
30	2	0.0246	109.53
32	2	0.0155	116.46
34	2	0.0198	123.47
36	2	0.0156	130.54
38	2	0.0133	137.48
40	2	0.0060	145.33
42	2	0.0037	151.75
44	2	0.0045	158.49
46	2	0.0043	165.82
48	2	0.0026	172.68
50	2	0.0015	179.49
50	8	0.2942	179.52
55	8	0.1964	197.32
60	8	0.2410	214.97
65	8	0.1808	232.16
70	8	0.2136	249.57
75	8	0.2365	267.26
80	8	0.1971	284.81
85	8	0.1371	302.60
90	8	0.1102	321.23
95	8	0.0785	337.47
100	8	0.0568	355.73
110	8	0.0199	390.02
120	8	0.0172	425.75
130	8	0.0128	461.36
140	8	0.0100	497.62
150	8	0.0046	531.28
160	8	0.0027	545.30

V. CONCLUSIONS

An optimized algorithm that approaches solutions for the forward Dirichlet boundary value problem, corresponding to the Impedance Equation in the plane, is an important contribution to the Electrical Impedance Tomography theory.

This is asserted by considering that the examples presented in this work, could well pose a difficult challenge if analysed with classical numerical methods, as the Finite Element variations are (see e.g. [6]).

In this sense, the optimized method can be used for analysing physical conductivity distributions, since no variations are needed for examining those cases when the exact mathematical expressions are unknown [10]. Furthermore, the results suggest that an adequately valance between the numerical accuracy and the computational cost has been achieved.

Note that it is still possible to improve the development of the method, by simply employing the available parallel computational techniques and devises. This, indeed, would significantly reduce the executions times, without provoking loss of precision or accuracy. Beside, many characteristics

ISBN: 978-988-19251-6-9
ISSN: 2078-0958 (Print); ISSN: 2078-0966 (Online)

discussed along these pages might be subjects of further works.

For example, the factor A, introduced in (20) to warrant the numerical stability of the method, was empirically approached during the experimental phase, but it was not possible to detect any pattern for predicting its magnitude, when only considering the conductivity distribution, or the domain.

Another question is why the total number of points $K+1$ per radius, did not have a strong influence in the obtained results, as it could have been expected. This immediately indicates that a larger number of experiments, employing different domains and boundary conditions, are necessary to understand the contribution of the $K+1$ points.

As a matter of fact, it is a very welcome opportunity for considering data obtained from physical measurements, locating the optimized method among the mathematical tools, employed for analysing the Electrical Impedance Tomography problem.

***Acknowledgements** 1:* The authors would like to acknowledge the support of CONACyT project 106722; C. M. A. Robles G. would like to thank the support of CONACyT project 81599 and of La Salle University for the research stay; A. Bucio would like to thank the support of CONACYT; and M.P. Ramirez T. thanks the support of HILMA S.A. de C.V.

REFERENCES

[1] K. Astala, L. Päivärinta (2006), *Calderon's inverse conductivity problem in the plane*, Annals of Mathematics, Vol. 163, pp. 265-299.

[2] L. Bers (1953), *Theory of Pseudoanalytic Functions*, IMM, New York University.

[3] A. Bucio R., R. Castillo-Perez, M.P. Ramirez T. and C. M. A. Robles G. (2012), *A Simplified Method for Numerically Solving the Impedance Equation in the Plane*, 9th International Conference on Electrical Engineering, Computing Science and Automatic Control (accepted for publication).

[4] A. Bucio R., R. Castillo-Perez, M.P. Ramirez T. (2011), *On the Numerical Construction of Formal Powers and their Application to the Electrical Impedance Equation*, 8th International Conference on Electrical Engineering, Computing Science and Automatic Control, IEEE Catalog Number: CFP11827-ART, ISBN:978-1-4577-1013-1, pp. 769-774.

[5] H. M. Campos, R. Castillo-Perez, V. V. Kravchenko (2011), *Construction and application of Bergman-type reproducing kernels for boundary and eigenvalue problems in the plane*, Complex Variables and Elliptic Equations, 1-38.

[6] R. Castillo-Perez., V. Kravchenko, R. Resendiz V. (2011), *Solution of boundary value and eigenvalue problems for second order elliptic operators in the plane using pseudoanalytic formal powers*, Mathematical Methods in the Applied Sciences, Vol. 34, Issue 4.

[7] V. V. Kravchenko (2009), *Applied Pseudoanalytic Function Theory*, Series: Frontiers in Mathematics, ISBN: 978-3-0346-0003-3.

[8] V. V. Kravchenko (2005), *On the relation of pseudoanalytic function theory to the two-dimensional stationary Schrödinger equation and Taylor series in formal powers for its solutions*, Journal of Physics A: Mathematical and General, Vol. 38, No. 18, pp. 3947-3964.

[9] M. P. Ramirez T. (2012), *Study of the forward Dirichlet boundary value problem for the two-dimensional Electrical Impedance Equation*, available in electronic at http://arxiv.org

[10] M. P. Ramirez T., R. A. Hernandez-Becerril, M. C. Robles G. (2011), *First characterization of a new method for numerically solving the Dirichlet problem of the two-dimensional Electrical Impedance Equation*, available in electronic at http://arxiv.org

[11] I. N. Vekua (1962), *Generalized Analytic Functions,* International Series of Monographs on Pure and Applied Mathematics, Pergamon Press.

[12] J. G. Webster (1990), *Electrical Impedance Tomography*, Adam Hilger Series on Biomedical Engineering.